JOURNAL OF VIROLOGY, Jan. 1993, p. 455–463
0022-538X/93/010455-09$02.00/0

Vol. 67, No. 1

Identification and Characterization of the p35 Gene of *Bombyx mori* Nuclear Polyhedrosis Virus That Prevents Virus-Induced Apoptosis

SHIZUO GEORGE KAMITA, KEI MAJIMA,† AND SUSUMU MAEDA*

Department of Entomology, University of California, Davis, California 95616

Received 21 August 1992/Accepted 14 October 1992

Nucleotide sequence analysis of the *Bombyx mori* nuclear polyhedrosis virus (BmNPV) genome revealed the existence of a gene homologous to the p35 gene of *Autographa californica* NPV (AcNPV), which has been shown to prevent virus-induced apoptosis. The BmNPV p35 gene showed 96.1% nucleotide and 89.6% predicted amino acid sequence identity to the AcNPV p35 gene. A mutant BmNPV (BmP35Z) lacking a functional p35 gene induced apoptosis-like cell degradation in infected BmN cells. However, unlike the p35-deleted AcNPV mutant (vAcAnh), BmP35Z replicated normally and produced polyhedral inclusion bodies. The patterns of protein synthesis and the percentages of viable BmN cells remaining following infection with either wild-type BmNPV or BmP35Z were nearly identical. BmP35Z also replicated in silkworm larvae without showing any apparent apoptotic response in infected hemocytes, fat body, or other tissues. Time to death of larvae infected with BmP35Z was similar to that for wild-type-infected larvae, and significant numbers of polyhedral inclusion bodies were produced. These results indicate that viral factors (or genes) other than p35 or host cell factors play a role in inducing, accelerating, or interfering with apoptotic processes. The evolution of baculovirus genomes is also discussed with reference to comparative analysis of the p35 and p94 gene sequences. The p94 gene is found immediately upstream of p35 in AcNPV; in BmNPV, however, the p94 gene was nearly completely missing, presumably because of large deletions in a BmNPV ancestor virus having a gene similar to the AcNPV p94 gene.

Nuclear polyhedrosis viruses (NPVs), a subfamily of the family *Baculoviridae*, are characterized as viruses with enveloped virions and circular double-stranded DNA genomes. Baculoviruses are currently used as efficient vectors for expression of foreign genes in insect cells and larvae (16, 17, 19, 27) and have potential for agricultural pest control (5), especially when speed of insect killing is increased by using recombinant DNA technology (25, 36, 37).

Gene expression of baculoviruses is temporally regulated during replication and is classified into at least three phases, immediate-early (or early), late, and very late (for a review, see reference 35). Immediate-early genes are transcribed by the host RNA polymerase II, while late and very late genes are believed to be transcribed by a virus-encoded RNA polymerase, which is α-amanitin resistant (8). Baculovirus genomes are considered to encode about 100 genes, and several viral structural and regulatory genes have been identified and characterized (35). *Autographa californica* NPV (AcNPV) is the best-characterized baculovirus at the molecular level. Recently, a gene (p35) which prevents virus-induced apoptosis has been found in the AcNPV genome by its accidental deletion during routine expression vector screening (2).

Apoptosis is thought to be an active, intrinsically programmed phenomenon that is involved in controlled, selective, and biologically meaningful deletion of cells (11). Apoptosis was observed in SF-21 cells infected with vAcAnh, a mutant AcNPV with a deletion in the p35 gene (2). The p35 gene of AcNPV is characterized as an immediate-early gene on the basis of its positive transcription in the presence of cycloheximide (4). Sequences between 55 and 155 bp upstream of the translational start of the AcNPV p35 gene are necessary for normal transcription during an immediate-early stage of infection (29). Deletion and site-directed mutagenesis experiments further indicate that GC and CGT motifs in a 60-bp region (between 30 and 90 bp from the transcriptional start) potentiate the basal promoter element (TATA box) that directs immediate-early gene transcription (3). The AcNPV p35 gene also possesses a TTAAG sequence 32 bp upstream of its translational start, which is a consensus sequence ([A/T/G/]TAAG) of baculovirus late gene promoters (31, 33, 34).

DNA hybridization and direct sequence analyses reveal that the gene organization of NPVs is conserved, although deletions, insertions, and/or inversions have been found in a few genes (for a review, see reference 1). The genomes of AcNPV and *Bombyx mori* NPV (BmNPV) (9, 10, 21, 22, 28) are highly homologous, as determined from genomic hybridization experiments (23) and direct sequence comparisons. However, BmNPV and AcNPV exhibit different phenotypic characteristics, such as host specificity (12). Given these unique characteristics, our group has studied the host range determinants of baculoviruses at the DNA level.

To study the mechanisms of baculovirus-induced apoptosis and its relationship to host specificity, a gene corresponding to AcNPV p35 was identified in the BmNPV genome by sequence analysis. The effects of the BmNPV p35 gene on BmNPV replication were examined both in vitro and in vivo, using a BmNPV mutant, BmP35Z, with a functionally inactive p35 gene. Apoptosis-like cell degradation was found in BmP35Z-infected BmN cells; however, this morphology was not detected in infected silkworm larvae. BmP35Z replication occurred normally both in the BmN cell line and in

* Corresponding author.
† Present address: Mitsubishi Kasei Institute of Life Sciences, Machida 194, Japan.

silkworm larvae. Furthermore, in BmN cell culture, the percentage of viable cells following infection with BmP35Z was nearly identical to that found following wild-type BmNPV infection.

MATERIALS AND METHODS

Cells, viruses, and silkworms. BmN cells were maintained in TC-100 supplemented with 10% fetal bovine serum as described previously (20, 24). The wild-type BmNPV isolate, BmNPV T3 (22), and BmP35Z were propagated in BmN. Viral infections were carried out by incubation at 27°C for 1 h at a multiplicity of infection (MOI) of 10. Viral growth curves were determined following infection of 4×10^6 BmN cells (in 5.0 ml of medium) with either BmP35Z or BmNPV T3. At appropriate times postinfection (p.i.), 100 μl of the culture supernatant was removed, centrifuged to remove cell debris, and stocked at −80°C prior to plaque assay. Plaque assay on BmN cells as described previously (20) was used to determine viral titers and to isolate p35-deleted BmNPVs following homologous recombination in cotransfected cells (20). Cell viability was determined by staining with 0.04% (final concentration) trypan blue in culture medium. Chromatin degradation was determined as described by Clem et al. (2).

Larvae of the silkworm *B. mori* were reared on artificial diet at 27°C (23). Synchronized fourth- and fifth-instar larvae were subjected to viral infection by injection of 10 μl of a viral suspension containing 5×10^5 PFU as described previously (20, 22). Production of polyhedra in larvae and cell morphology of infected hemocytes, fat body, and other tissues were examined with a light microscope after dissection and bleeding at 24-h intervals.

Identification and sequencing of the BmNPV p35 gene. The BmNPV p35 gene was speculated to be located in the BmNPV *Bam*HI D fragment (see below). To determine the nucleotide sequence of *Bam*HI-D, either the entire *Bam*HI D fragment or a part of it was inserted adjacent to a nonessential lambda DNA fragment, which was inserted into the multiple cloning region of a pUC-derived plasmid (pTZ18R; Pharmacia LKB, Piscataway, N.J.). Following cleavage at the *Bam*HI D fragment-lambda DNA junction, nested deletions of *Bam*HI-D were made by treatment with BAL 31 for up to 5 min at 31°C. The remaining lambda DNA was then removed (usually by cleavage with *Sma*I), and the plasmid backbone containing the *Bam*HI D fragment with nested deletions was self-ligated and transformed into competent *Escherichia coli* cells. Plasmids of appropriate size for sequencing were propagated, isolated, and sequenced by using an appropriate pUC primer by the dideoxy-chain termination method as described previously (21). The structure of a typical plasmid is represented by pBd20a in Fig. 1. Nucleotide sequencing data were analyzed on a microcomputer, using the DNASIS and PROSIS programs (Hitachi America, San Bruno, Calif.) as described previously (21).

Isolation of a BmNPV mutant with a deletion in the p35 gene. The p35 gene of BmNPV was inactivated by homologous recombination of wild-type BmNPV DNA with a plasmid, pP35LacZ, containing a β-galactosidase gene driven by a *Drosophila* heat shock promoter (*hsp70*) (Fig. 1). The *hsp70* promoter was used because of its relatively strong promoter activity in lepidopteran cell lines regardless of heat induction (38). The strategy for construction of pP35LacZ is shown in Fig. 1. Recombinant DNA techniques (restriction endonuclease cleavage, ligation, transformation, plasmid propagation, etc.) used in the constructions were performed

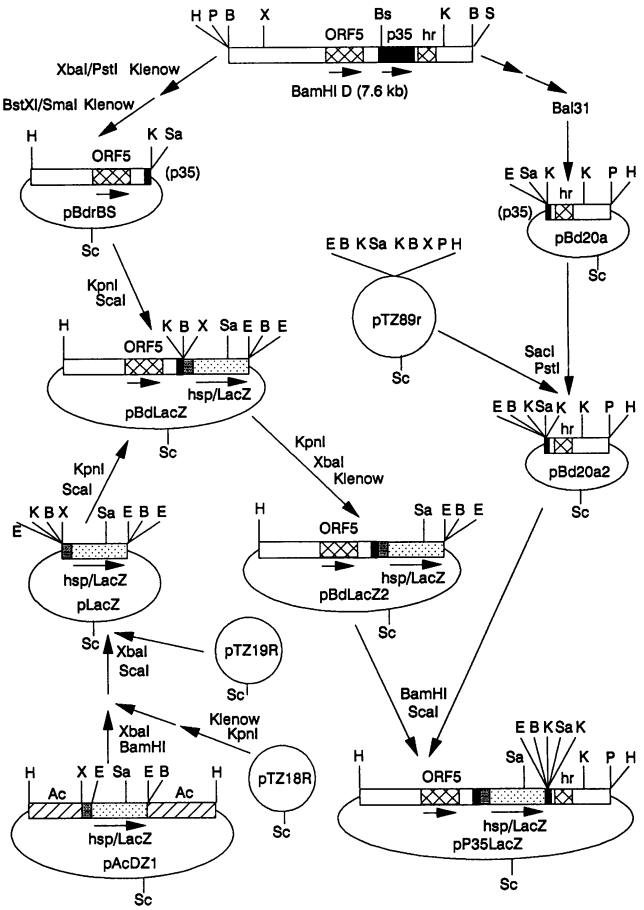

FIG. 1. Construction of pP35LacZ. The strategy used is described in Materials and Methods. A curved line represents the pTZ18R or pTZ19R plasmid backbone; inserted DNA fragments are represented by rectangles. DNA fragments: AcNPV polyhedrin flanking region (Ac; hatched); ORF5 (cross-hatched), p35 gene (black), the homologously repeated sequence hr5 (cross-hatched); hsp/LacZ; and the *hsp70*/β-galactosidase cassette (heavy stippling for the *hsp70* promoter and light stippling for the β-galactosidase coding region). Sequences other than the p35 and ORF5 coding regions and hr5 are indicated by unshaded rectangles. Arrows below the rectangles indicate directions of gene transcription. Restriction endonuclease recognition sites: H, *Hin*dIII; P, *Pst*I; B, *Bam*HI; X, *Xba*I; K, *Kpn*I; S, *Sma*I; E, *Eco*RI; Sa, *Sac*I; Sc, *Sca*I; Bs, *Bst*XI.

by using standard procedures as described previously (21, 23, 25, 26). All of the constructions were based on the pUC-derived plasmids pTZ18R and pTZ19R (Pharmacia LKB). The constructions were performed as follows. (i) The *hsp70*/β-galactosidase gene cassette was excised from pAcDZ1 (38), which was kindly provided by J. M. Vlak and D. Zuidema, Agricultural University Wageningen, Wageningen, The Netherlands, by cleavage with *Xba*I and *Bam*HI and transferred into the *Xba*I and *Bam*HI sites of pTZ18R, which was modified by removal of the *Kpn*I site (by digestion of *Kpn*I followed by treatment with the Klenow fragment of DNA polymerase I). This plasmid containing the *hsp70*/β-galactosidase cassette was then cleaved with *Xba*I and *Sca*I (in the ampicillin resistance gene) and ligated to the *Xba*I and *Sca*I sites in pTZ19R to generate pLacZ. (ii) A plasmid containing the entire 7.6-kbp *Bam*HI D fragment (23) was cleaved with *Xba*I (81.9 map units [m.u.]; Fig. 2B)

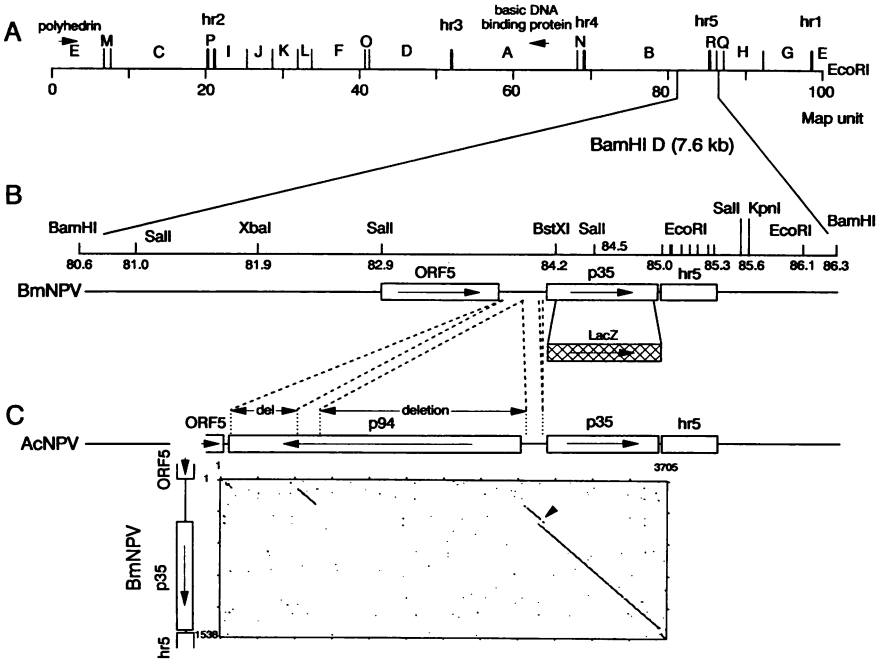

FIG. 2. Locations and comparison of the p35 genes of BmNPV and AcNPV. (A) Physical map of the BmNPV T3 genome for the restriction endonuclease *Eco*RI. Locations of homologously repeated (hr) regions and ORF5 are indicated above the map. Map position 0 is at the left end of the *Pst*I F fragment (23). (B) Physical map of the *Bam*HI D fragment (80.6 to 86.3 m.u.) and gene arrangement of the BmNPV p35 gene and flanking regions. The locations of the two large deletions and insertion (compared with the corresponding region in AcNPV) are shown by the dotted lines. The location of the *hsp70*/β-galactosidase cassette (cross-hatched rectangle) insertion in BmP35Z is also shown. (C) Nucleotide sequence homology dot plot analysis of the BmNPV and AcNPV p35 genes and flanking regions. A single dot indicates more than 12 identical nucleotides within 15-nt sequences. The arrowhead indicates duplication around the 5′ nontranslated region of the BmNPV p35 gene.

and *Pst*I (in the polylinker adjacent to the *Bam*HI site [80.6 m.u.]), treated with the Klenow fragment, and self-ligated in order to remove the *Bam*HI and *Xba*I sites (80.6 and 81.9 m.u.). The resultant plasmid was then digested with *Bst*XI (80 nucleotides [nt] downstream of the p35 translational start) and *Sma*I (in the polylinker adjacent to the *Bam*HI site [86.3 m.u.]) to delete most of the p35 gene coding region and downstream sequences (84.2 to 86.3 m.u.), treated with the Klenow fragment, and self-ligated to obtain pBdrBS. (iii) pLacZ and pBdrBS were combined by digestion and ligation at the *Kpn*I and *Sca*I sites to form pBdLacZ. The *Bam*HI site between the *Kpn*I and *Xba*I sites in pBdLacZ was removed by *Kpn*I and *Xba*I digestion followed by treatment with the Klenow fragment to form pBdLacZ2. (iv) pBd20a (originally constructed by subcloning and BAL 31 treatment for nucleotide sequencing as described above), which contains sequences starting 39 bp upstream from the termination signal of the p35 gene to the 86.3 m.u. *Bam*HI site, was cleaved with *Pst*I and *Sac*I (in the polylinker) and transferred to a pUC-derived plasmid, pTZ89r, with a modified polylinker (*Eco*RI, *Bam*HI, *Kpn*I, *Sac*I, *Kpn*I, *Bam*HI, *Xba*I, *Pst*I, and *Hin*dIII) to generate pBd20a2. Plasmid pTZ89r was constructed by *Sac*I and *Kpn*I digestion of pTZ19R followed by Klenow treatment, *Bam*HI and *Sca*I cleavage followed by ligation to the *Bam*HI and *Sca*I sites in pTZ18R, and *Sac*I and *Sca*I digestion followed by ligation to the *Sac*I and *Sca*I sites of pTZ19R. (v) pBdLacZ2 and pBd20a2 were cleaved with *Bam*HI and *Sca*I and ligated to obtain pP35LacZ, which contained the *hsp70*/β-galactosidase cassette in the coding region of the p35 gene along with 2.9 kbp of the 5′ and 1.8 kbp of the 3′ regions of the p35 gene.

Protein labeling and SDS-PAGE. Replicate plates of BmN cells (1.2×10^6 cells per 35-mm-diameter dish) were infected with either BmP35Z or BmNPV T3 to examine protein synthesis. At the appropriate times p.i., the cells were washed once with methionine-free TC-100 containing 1% fetal bovine serum and pulse-labeled with 10 μCi of L-[^{35}S]methionine per 200 μl of methionine-free medium per 35-mm-diameter dish for 30 min. Following labeling, cells were collected by centrifugation (200 × *g*, 5 min), washed once with phosphate-buffered saline, and stored at −80°C until use. Cell pellets were dissolved in 100 μl of sample buffer, and 7 μl was subjected to sodium dodecyl sulfate-polyacrylamide gel electrophoresis (SDS-PAGE) as described by Laemmli (13), using 10% acrylamide gels (0.4% bisacrylamide). Gels were treated with an enhancer, Resolution (EMCorp, Chestnut Hill, Mass.), under conditions recommended by the manufacturer, dried under vacuum on gel blotting paper, and exposed to Kodak XAR X-ray film (Eastman Kodak Co., Rochester, N.Y.).

Nucleotide sequence accession number. The nucleotide sequence reported in this article can be obtained from GenBank. The accession number is L04802.

RESULTS

Identification of the BmNPV p35 gene. The existence of a gene in the BmNPV genome having high nucleotide sequence homology to the AcNPV p35 gene was confirmed by a homology search of sequence data obtained by random cloning and sequencing of the BmNPV genome (21). From the high homology between the BmNPV and AcNPV ge-

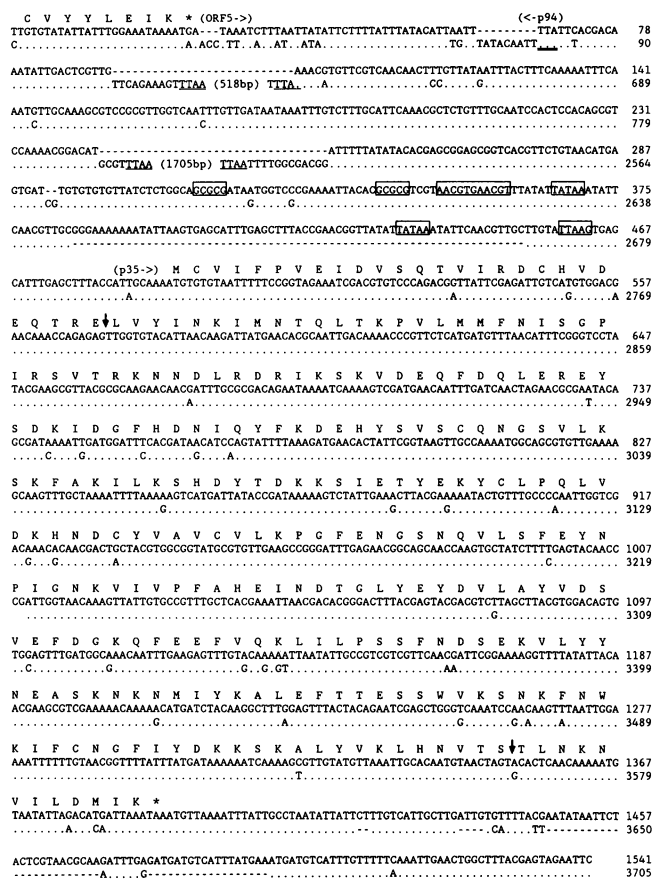

FIG. 3. Nucleotide sequence and deduced amino acid sequence of the BmNPV p35 gene region. The nucleotide sequence of the corresponding AcNPV region is shown below the BmNPV p35 nucleotide sequence. A dot indicates an identical nucleotide, and a dash indicates a deletion (or no corresponding nucleotide). The deduced amino acid sequence of BmNPV p35 and the 3′ end of ORF5 are shown above the corresponding nucleotide sequence. The GC, CGT, and TATA box motifs and consensus baculovirus late gene promoter sequence in BmNPV are boxed. The stop codon of the AcNPV p94 gene (4) is doubly underlined, and the TTAA sequences are underlined. The arrows indicate the positions of the *hsp70*/β-galactosidase cassette insertion.

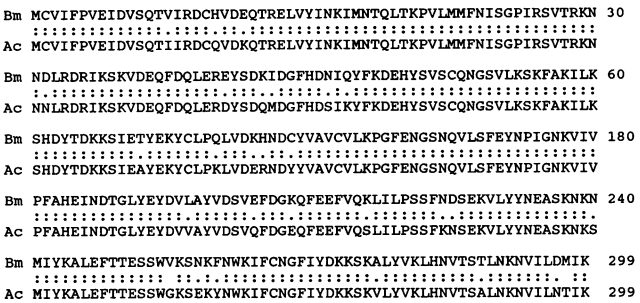

FIG. 4. Comparison of the deduced amino acid sequences of BmNPV p35 (Bm) and AcNPV p35 (AC) (4). The deduced amino acid sequences are represented in single-letter code. Two dots indicate an identical amino acid, and a single dot indicates an amino acid with similar characteristics.

nomes (24), the BmNPV p35 gene was then speculated to be located in the BmNPV *Bam*HI D fragment (80.6 and 86.3 m.u.) of BmNPV (23). Following direct sequencing of this fragment, the precise position of the BmNPV p35 gene was mapped to between 84.1 and 84.9 m.u. on the BmNPV map (23) (Fig. 2A and B). A physical map of *Bam*HI-D for several restriction endonucleases is shown in Fig. 2B. Homology analysis of the p35 genes and flanking regions of BmNPV and AcNPV is shown in Fig. 2C. In this region (BmNPV 82.9 to 85.4 m.u.), AcNPV has three open reading frames (ORFs) (ORF5, p94, and p35) (4, 30) and a region of homologously repeated sequences (hr5) (6, 14). In BmNPV, sequences corresponding to ORF5, p35, and hr5 were found (Fig. 2B and C; data not completely shown); however, most sequences corresponding to the p94 gene were missing (Fig. 2B and C).

Sequence analysis of the BmNPV p35 gene. Figure 3 shows the nucleotide sequence of the BmNPV p35 gene and flanking sequences along with the corresponding AcNPV sequence (4). Both the BmNPV and AcNPV p35 ORFs are 897 bp long. A 65-bp insertion, which seemed to be caused by partial duplication (arrowhead in Fig. 2C; Fig. 3), was found between 37 and 102 bp upstream of the putative translational start of the BmNPV gene. This insertion resulted in an additional TATA box 56 bp upstream of the putative translational start of the BmNPV p35 gene. Because of the duplicative nature of this insertion, it was also possible to consider the insertion as occurring between 62 and 121 bp upstream of the putative translational start, in which case the additional TATA box would be located 121 bp upstream of the putative translational start. Consensus GC, CGT, and TATA motifs sufficient for immediate-early gene expression (3) were found upstream of this insertion at positions identical to those found in the upstream region of the AcNPV p35 gene. Excluding this insertion, the 5′ flanking region (between nt 293 and 490 in Fig. 3) of the BmNPV p35 gene was nearly identical (97.2%) to the corresponding AcNPV region (Fig. 3). A typical baculovirus immediate-early gene motif (TATA/CAGT) (1), however, was not found in the 5′ region. A TTAAG sequence was found 32 bp upstream (nt 459 in Fig. 3) of the putative translational start site of the BmNPV p35 gene at a position identical to that of AcNPV p35.

The 3′ regions of the BmNPV and AcNPV p35 genes were about 95.4% conserved (excluding deletions). A putative poly(A) signal was found in BmNPV at a position (nt 1386 in Fig. 3) which was identical to that of the AcNPV p35 gene (4).

The nucleotide sequence of the BmNPV p35 gene showed 96.1% sequence identity to the AcNPV p35 gene (Fig. 3). Thirty-five nucleotide substitutions between the BmNPV and AcNPV p35 genes generated 28 amino acid substitutions, resulting in 89.6% amino acid sequence identity (Fig. 3 and 4). Two of the 28 amino acid substitutions in BmNPV p35 resulted in amino acids with characteristics significantly different from those of AcNPV p35 (Fig. 4). The predicted BmNPV p35 protein was 298 amino acids in length with an estimated molecular mass of 34,779 Da. Hydrophobic secretion and membrane-anchoring sequences were not found. The amino acid substitutions appeared to occur randomly, although substitutions were not found in amino acids 13 to 61, 95 to 131, and 149 to 195 (Fig. 4).

Sequence analysis of p94. Homology dot plot analysis indicated that two large deletions of 1,730 and 536 bp occurred in the region of the BmNPV genome corresponding to the AcNPV p94 gene (Fig. 2C). These deletions were separated by 151 bp of sequence with high (96.1%) homology

to the corresponding 151-bp sequence in the coding region of the AcNPV p94 gene. The 1,730-bp deletion was found 242 bp upstream of the putative translational start of BmNPV p35 (nt 245 in Fig. 3) and corresponded to about three-fourths of the AcNPV p94 gene coding region beginning 31 bp upstream of the AcNPV p94 gene translational start (Fig. 2C). The 536-bp deletion was found 393 bp upstream of the putative translational start site of BmNPV p35 (nt 94 in Fig. 3), i.e., immediately downstream of the 151-bp homologous sequence (Fig. 3), and ended 24 bp before the translational stop of the AcNPV p94 gene (Fig. 2C and 3). No apparent ORFs were identified in this region of BmNPV in either direction. Comparative sequence analysis of the BmNPV and AcNPV p94 gene regions indicated that TTAA sequences were found within 13 bp of both ends of the two large deletions. TTAA sequences have been shown to be involved in spontaneous insertion into the viral genome of heterologous DNA fragments from the host cell or other viral DNA fragments following cotransfection (for a review, see reference 1). When nucleotide sequences corresponding to the hypothesized deletions were searched for in a BmNPV nucleotide sequence data bank (18, 21) covering most of the BmNPV genome, no apparent homology was found.

Deletion of the p35 gene from the BmNPV genome. To characterize the p35 gene of BmNPV, 87% of the p35 coding region was deleted (Fig. 2B; arrows in Fig. 3) by homologous recombination in cotransfected BmN cells. The percentage (0.5%) of p35-deleted viruses (plaques stained blue) was similar to the percentage of recombinant viruses generated in cotransfection experiments in which the polyhedrin gene is replaced by a foreign gene construct. Following three rounds of plaque purification, three independent clones were isolated and characterized. Since the three clones did not show any apparent phenotypic differences, clone 1 (designated BmP35Z) was used in further experiments.

During plaque purification of BmP35Z, two interesting phenomena were observed. First, BmN cells infected with BmP35Z showed apoptosis-like cell degradation and low production of polyhedral inclusion bodies (PIBs) in comparison with wild-type-infected cells. Second, plaques formed by BmP35Z-infected BmN cells appeared to produce larger areas of blue staining when overlaid with 5-bromo-4-chloro-3-indolyl-β-D-galactopyranoside (X-Gal) containing agarose than did plaques formed by cells infected with other recombinant BmNPVs carrying the same *hsp70*/β-galactosidase gene cassette (when inserted into the hr5 region or ecdysteroid UDP glucosyltransferase gene of BmNPV [18]). When observed under light microscopy, cells distal to the center of the plaque appeared to be uninfected; they were, however, stained blue, indicating that β-galactosidase was synthesized and rapidly released, possibly as a result of lysis of apoptotic bodies. However, when plaques were visualized with an overlay containing neutral red, the actual plaque area (nonstained, dead cells) was the same as in other BmNPV-formed plaques (data not shown).

Infection of BmP35Z in BmN cells. Light microscopic observation revealed gross morphological differences in mock-infected and virus (BmP35Z and BmNPV T3)-infected BmN cultures by 24 h p.i. (Fig. 5). Cytopathic effects typical of normal baculoviral infection were observed in both infections beginning around 10 h p.i.; the morphology of BmN cells infected with either virus was indistinguishable prior to 16 h p.i. By 17 h p.i., small protrusions which eventually matured into apoptotic bodies were seen in less than 1% of BmP35Z-infected cells. By 24 h p.i., this process intensified and at least 10% of the BmP35Z-infected cells were in some stage of blebbing (Fig. 5D), which is a characteristic of the initial phase of apoptosis (11). By 36 h p.i., about 15% of BmP35Z-infected cells were blebbing, and immature PIBs were faintly visible in about 5% of the cells. Cell aggregation was also observed; however, aggregation was apparent only in completely undisturbed cultures because of the weak attachment of infected BmN cells to the culture surface after about 36 h p.i. By 48 h p.i., the proportion of blebbing cells increased to about 30%, and mature PIBs were seen in about 10% of the cells (Fig. 5F). By 72 h after BmP35Z infection, mature PIBs were observed in about 20% of the cells, and about 70% of the cells appeared to have gone through the blebbing process (or were in the process of blebbing). Cell debris and free PIBs indicative of cell lysis or rupture were also observed (Fig. 5H).

The blebbing process was not observed in wild-type-infected cells at any time during the infection cycle (Fig. 5C, E, and G). In BmNPV T3-infected cells, immature PIBs were observed in about 25% of cells at 36 h p.i. The percentage of BmNPV T3-infected cells showing PIBs progressively increased until 72 h p.i., at which time PIBs were observed in greater than 90% of the cells (Fig. 5E and G).

The blebbing process was not uniform. Some cells were able to form spherical subcellular (apoptotic) bodies in less than 1 h following the initial observation of blebbing, while other cells were not able to pinch off the apoptotic bodies, which subsequently elongated and remained attached to the mother cell for periods of over 12 h. Still other cells formed numerous smaller spherical bodies, while others formed only one or two larger ones. All of the apoptotic bodies were morphologically distinct from the infected cells; they were very smooth and translucent, and they excluded trypan blue. Regardless of the number or type of subcellular bodies formed, most cells that underwent the blebbing process did not appear to completely disintegrate (48 h p.i.), and a small core of cellular mass including an apparently intact nuclear membrane remained. This core cell was generally more damaged in appearance than were BmNPV T3-infected cells but was still able to exclude trypan blue. The percentages of trypan blue-excluding cells remaining following infection with either BmP35Z or BmNPV T3 were nearly identical prior to 48 h p.i., at which time about 70% of cells infected with either virus excluded trypan blue. At 36 h p.i., Clem et al. (2) found about 98% viability in wild-type AcNPV-infected SF-21 cells and less than 7% viability in vAcAnh-infected SF-21 cells, as judged by trypan blue exclusion. Furthermore, chromatin degradation was not observed in BmP35Z- or BmNPV T3-infected BmN cells at 48 h p.i. (data not shown).

The viral growth curve of BmP35Z was very similar to that of BmNPV T3 (Fig. 6). Both viruses reached a plateau maximum of about 2×10^8 PFU/ml at about 48 h p.i. However, between 12 and 36 h p.i., BmP35Z seemed to replicate more slowly than did BmNPV T3.

Protein synthesis of BmP35Z-infected cells. Protein synthesis in infected cells, which can be an indicator of cell viability, was examined at various times p.i. by SDS-PAGE following pulse-labeling. The pattern of protein synthesis in BmP35Z-infected BmN cells was very similar to that of BmNPV T3-infected BmN cells (Fig. 7). By 12 h p.i., several putative virus-specific bands were observed, and beginning around 24 h p.i., suppression of host protein synthesis was recognized. At a late stage of infection (36, 48, and 72 h p.i.), a major 30-kDa protein was detected and host protein synthesis was dramatically attenuated. The 30-kDa protein synthesized during a late stage of infection was most likely

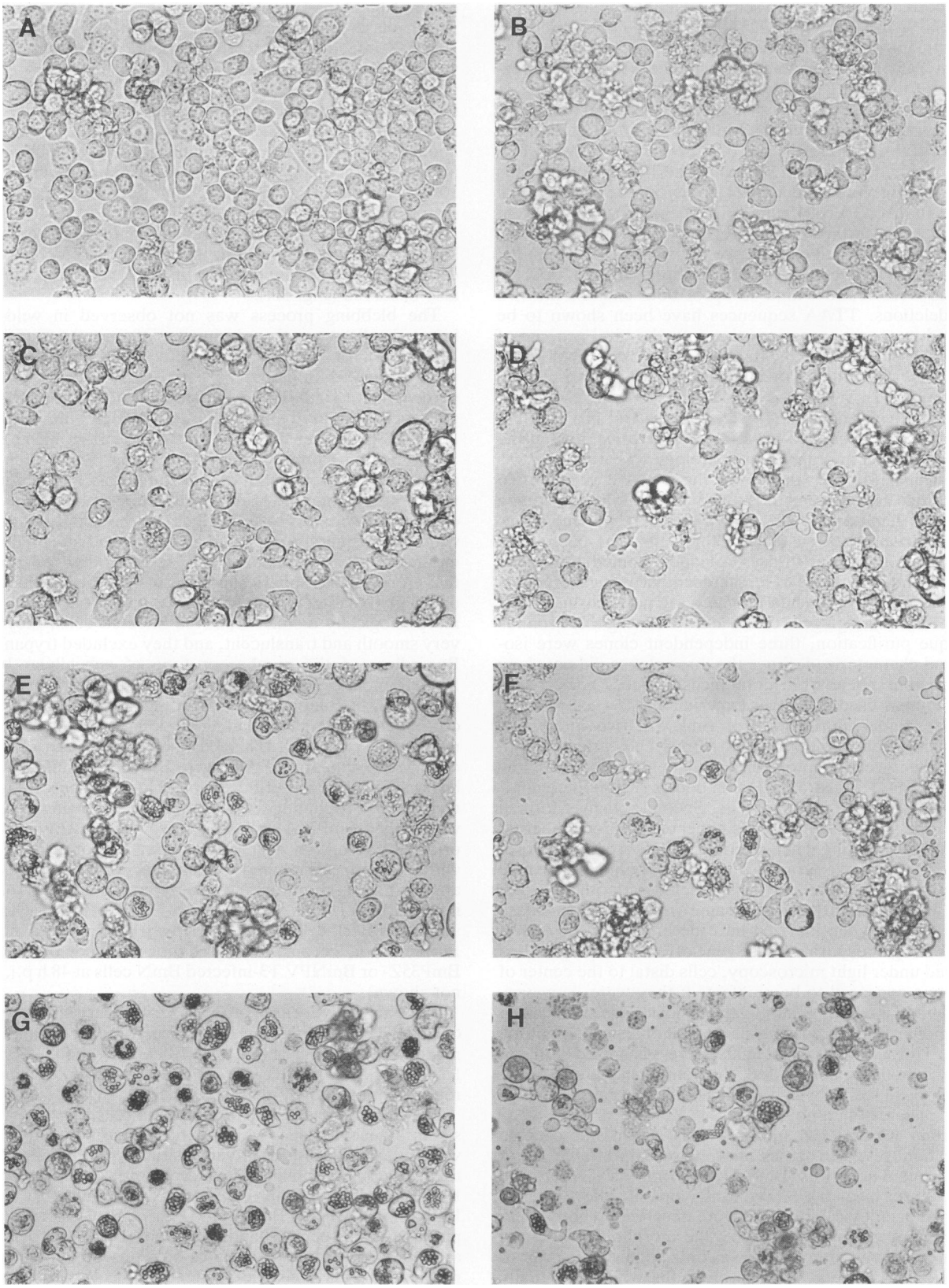

FIG. 5. Light microscopy of BmN cells infected (MOI of 10) with BmP35Z (B, D, F, and H) or BmNPV T3 (C, E, and G) or mock infected (A) (magnification, ×400). Cells were observed at 24 (A to D), 48 (E and F), or 72 (G and H) h p.i. Cells observed at 48 and 72 h p.i. were detached from the culture surface and are not necessarily indicative of the true cell numbers.

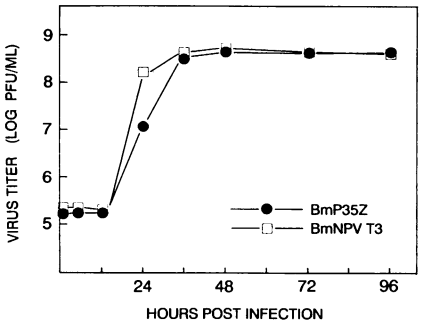

FIG. 6. Growth curves of BmP35Z and BmNPV T3. BmN cells were infected with virus at an MOI of 10 and incubated at 27°C. At 1, 5, 12, 24, 36, 48, and 72 h p.i., 100 μl of culture supernatant was collected, and viral titers were determined by plaque assay on BmN cells as described in Materials and Methods.

polyhedrin, as judged from its estimated molecular weight and extremely high expression. This conclusion was confirmed by Coomassie brilliant blue staining and analysis with a polyhedrin-deficient BmNPV mutant (data not shown). In general, protein synthesis appeared more retarded in BmP35Z-infected cells beginning at a late stage of infection. In particular, polyhedrin was detected at less than one-third of the levels of BmNPV T3-infected cells 36, 48, and 72 h p.i.

Effects of BmP35Z infection in silkworm larvae. The ability of BmP35Z to induce apoptosis was also examined in tissues of the silkworm. Major differences were not detected between silkworm larvae infected with either BmP35Z or BmNPV T3. Synchronized fourth (day 3)- or fifth (day 2)-instar silkworm larvae injected with either virus died between 4 and 5 days or 5 and 6 days postinjection, respectively. Apoptosis-like cell morphology was not detected in any tissues at any time after injection of either virus. At 2 days postinjection, PIB production was observed in the hemocytes of both fourth- and fifth-instar larvae injected with either virus. It also appeared that fewer PIBs were produced in the hemocytes of BmP35Z-infected larvae at 2 days postinjection (data not shown). By 4 or 5 days postinjection, similar amounts of free PIBs and cell debris, including lysed fat body cell components, were seen in the hemolymph of larvae infected by either virus.

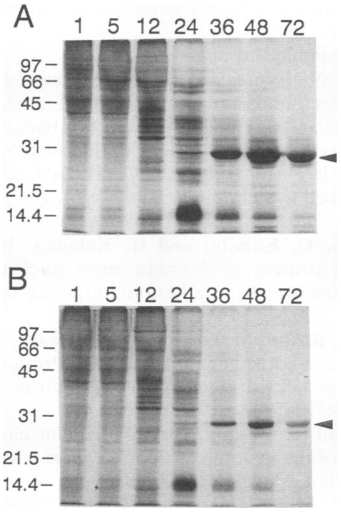

FIG. 7. SDS-PAGE of pulse-labeled proteins of BmN cells infected with either BmNPV T3 (A) or BmP35Z (B) at 1, 5, 12, 24, 36, 48, or 72 h p.i. The arrowhead indicates polyhedrin. Molecular masses in kilodaltons are indicated at the left.

DISCUSSION

We have identified a BmNPV gene with high nucleotide (96.1%) and predicted amino acid (89.6%) sequence homology to the AcNPV p35 gene. Infection of BmN cells with BmP35Z induced changes in cell morphology which were similar to those observed during the initial stages of apoptosis induced by vAcAnh in SF-21 cells (2). The response of BmN to BmP35Z infection indicates that BmNPV p35 can prevent at least the initial stages of apoptosis; however, in marked contrast to vAcAnh-infected SF-21 cells, completion of the apoptotic response (ending in cell death) did not occur in BmN cells infected with BmP35Z. BmP35Z replicated normally in BmN cells and produced polyhedra in 20% of the infected cells. Furthermore, protein synthesis patterns between BmP35Z- and BmNPV T3-infected cells were similar, and BmP35Z and BmNPV T3 killed infected larvae at similar rates.

The different responses of BmN and SF-21 cells infected by BmP35Z and vAcAnh, respectively, may be the result of differences in viral factors and/or host cell factors (genes) related to the apoptotic response. Evidence for the existence of viral factors, which act either directly or indirectly, include the findings that (i) apoptosis is initiated by BmP35Z and vAcAnh infection and (ii) differential apoptotic responses are induced in BmN cells by vAcAnh (2) and BmP35Z. Evidence for the existence of host factors include the findings that (i) SF-21 and *Trichoplusia ni* cells infected with vAcAnh responded differently (2, 7), (ii) *B. mori* larvae infected with BmP35Z did not show any apoptotic response, and (iii) the apoptotic response was not uniform in BmP35Z-infected BmN cells and vAcAnh-infected SF-21 cells (2). This evidence suggests several explanations for why BmP35Z infection of BmN cells does not induce complete apoptosis: (i) viral factors which lead to cell death are not as active or are missing in BmNPV, (ii) there are viral factors other than p35 which can prevent apoptosis during BmNPV infection, (iii) host cell factors which block or shut off apoptosis are different in BmN cells, and (iv) BmN cells are able to recover from apoptosis induction in the absence of p35.

A synchronous apoptotic response was never observed in BmN cell cultures infected with BmP35Z. At 72 h after BmP35Z infection, only 70% of the infected cells showed an apoptotic response, while about 20% showed typical polyhedral production which was generally indistinguishable from that of BmN cells infected with BmNPV T3. These percentages did not change significantly in repeat experiments and in experiments in which the MOI was changed (data not shown). These phenomena strongly suggest the existence of a host factor(s) preventing initiation of apoptotic processes whose expression is coupled with the host cell cycle.

B. mori larvae infected with either BmP35Z or BmNPV T3 were morphologically indistinguishable. In mammalian tissues, apoptotic bodies are usually rapidly phagocytosed and degraded by neighboring cells so that the apoptotic event is not easily seen (11); this may have also been the case for BmP35Z-infected silkworm larvae. BmP35Z- and BmNPV T3-infected larvae also did not show significant differences in

terms of time to death, indicating that cellular factors may have been able to suppress apoptosis in the absence of the BmNPV p35 gene. In invertebrate organisms, extracellular regulators such as hormones have been shown to play a critical role in apoptosis associated with reproduction and metamorphosis (15).

The promoter regions between the p35 genes of BmNPV and AcNPV were very similar except for a 65-bp insertion by partial duplication (Fig. 2C and 3). This insertion placed the putative transcriptional start site of the BmNPV p35 gene 65 bp upstream of the one found in AcNPV; however, it did not disturb the relative positions of the GC, CGT, and TATA box motifs. Transcription at an early stage of infection is expected to occur at 29 to 34 bp downstream of this TATA box (3), resulting in a BmNPV transcript that is 47 to 52 nt longer than the corresponding AcNPV transcript. Sequences (about 30 bp) upstream and downstream of the baculovirus late gene promoter motif (TTAAG) were nearly identical to the corresponding sequences of AcNPV.

The 96.1% nucleotide and 89.6% amino acid sequence identities shown by the p35 genes of BmNPV and AcNPV indicate that codon usage changes occurred relatively frequently (28 of the 35 nucleotide substitutions) in the p35 gene. This finding was comparable to the nucleotide and amino acid sequence identities of other BmNPV and AcNPV genes, including those encoding the basic DNA-binding protein (95.3% nucleotide and 94.6% amino acid sequence conservation) (21), p40 (94 and 94.4%) (39), IE-1 (95.3 and 95.5%) (9), ORF1629 (95.6 and 90.4%) (10, 18, 32), and polyhedrin (77.0 and 86.1%) (10, 22).

Almost all sequences corresponding to the p94 gene region of AcNPV were missing in BmNPV as a result of two large deletions. The deletions were hypothesized on the fact that a 151-bp fragment with high (96%) homology (without insertions and deletions) to AcNPV p94 was retained in a region between the p35 and ORF5 genes of BmNPV which corresponds to the location of the AcNPV p94 gene. These results indicate that the putative deletions occurred recently in the evolutionary history from an ancestor gene similar to the AcNPV p94 gene.

BmNPV and AcNPV have high genome homology (24) yet exhibit completely different host specificity characteristics. We have previously shown that because of this high homology, recombination occurs frequently between BmNPV and AcNPV in coinfected SF-21 cells (12). Studies of apoptotic processes in two different host cells, BmN and SF-21, using BmNPV and AcNPV recombinant viruses with and without the p35 gene will allow the identification of viral genes or host cell factors that are involved in apoptosis. These types of studies will also be of interest with regard to understanding host defense mechanisms against viral infection, host specificity determinants, and replication strategies of baculoviruses in general.

REFERENCES

1. **Blissard, G. W., and G. F. Rohrmann.** 1990. Baculovirus diversity and molecular biology. Annu. Rev. Entomol. **35**:127–155.
2. **Clem, R. J., M. Fechheimer, and L. K. Miller.** 1991. Prevention of apoptosis by a baculovirus gene during infection of insect cells. Science **254**:1388–1390.
3. **Dickson, J. A., and P. D. Friesen.** 1991. Identification of upstream promoter elements mediating early transcription from the 35,000-molecular-weight protein gene of *Autographa californica* nuclear polyhedrosis virus. J. Virol. **65**:4006–4016.
4. **Friesen, P. D., and L. K. Miller.** 1987. Divergent transcription of early 35- and 94-kilodalton protein genes encoded by the *Hin*dIII K genome fragment of the baculovirus *Autographa californica* nuclear polyhedrosis virus. J. Virol. **61**:2264–2272.
5. **Granados, R. R., and B. A. Federici.** 1986. The biology of baculoviruses, vol. I and II. CRC Press, Boca Raton, Fla.
6. **Guarino, L. A., and M. D. Summers.** 1986. Interspersed homologous DNA of *Autographa californica* nuclear polyhedrosis virus enhances delayed-early gene expression. J. Virol. **60**:215–223.
7. **Hershberger, P. A., J. A. Dickson, and P. D. Friesen.** 1992. Site-specific mutagenesis of the 35-kilodalton protein gene encoded by *Autographa californica* nuclear polyhedrosis virus: cell line-specific effects on virus replication. J. Virol. **66**:5525–5533.
8. **Huh, N. E., and R. F. Weaver.** 1990. Identifying the RNA polymerases that synthesize specific transcripts of the *Autographa californica* nuclear polyhedrosis virus. J. Gen. Virol. **71**:195–201.
9. **Huybrechts, R., L. Guarino, M. van Brussel, and V. Vulsteke.** 1992. Nucleotide sequence of a transactivating *Bombyx mori* nuclear polyhedrosis virus immediate early gene. Biochim. Biophys. Acta **1129**:328–330.
10. **Iatrou, K., K. Ito, and H. Witkiewicz.** 1985. Polyhedrin gene of *Bombyx mori* nuclear polyhedrosis virus. J. Virol. **54**:436–445.
11. **Kerr, J. F. R., J. Searle, B. V. Harmon, and C. J. Bishop.** 1987. Apoptosis, p. 93–128. *In* C. S. Potten (ed.), Perspectives on mammalian cell death. Oxford University Press, New York.
12. **Kondo, A., and S. Maeda.** 1991. Host range expansion by recombination of the baculoviruses *Bombyx mori* nuclear polyhedrosis virus and *Autographa californica* nuclear polyhedrosis virus. J. Virol. **65**:3625–3632.
13. **Laemmli, U. K.** 1970. Cleavage of structural proteins during the assembly of the head of bacteriophage T4. Nature (London) **227**:680–685.
14. **Liu, A., J. Qin, C. Rankin, S. E. Hardin, and R. F. Weaver.** 1987. Nucleotide sequence of a portion of the *Autographa californica* nuclear polyhedrosis virus genome containing the EcoRI site-rich region (hr5) and an open reading frame just 5′ of the p10 gene. J. Gen. Virol. **67**:2565–2570.
15. **Lockshin, R. A.** 1985. Programmed cell death, p. 301–317. *In* G. A. Kerkut and L. I. Gilbert (ed.), Comprehensive insect physiology, biochemistry, and pharmacology, vol. 2. Pergamon Press, Elmsford, N.Y.
16. **Luckow, V. A.** 1991. Cloning and expression of heterologous genes in insect cells with baculovirus vectors, p. 97–152. *In* A. Prokop, R. K. Bajpai, and C. S. Ho (ed.), Recombinant DNA technology and application. McGraw-Hill, Inc., New York.
17. **Luckow, V. A., and M. D. Summers.** 1988. Trends in the development of baculovirus expression vectors. Bio/Technology **6**:47–55.
18. **Maeda, S.** Unpublished data.
19. **Maeda, S.** 1989. Expression of foreign genes in insects using baculovirus vectors. Annu. Rev. Entomol. **34**:351–372.
20. **Maeda, S.** 1989. Gene transfer vectors of a baculovirus, *Bombyx mori* nuclear polyhedrosis virus, and their use for expression of foreign genes in insect cells, p. 167–181. *In* J. Mitsuhashi (ed.), Invertebrate cell system applications, vol. I. CRC Press, Boca Raton, Fla.
21. **Maeda, S., S. G. Kamita, and H. Kataoka.** 1991. The basic DNA-binding protein of *Bombyx mori* nuclear polyhedrosis virus: the existence of an additional arginine repeat. Virology **180**:807–810.
22. **Maeda, S., T. Kawai, M. Obinata, H. Fujiwara, T. Horiuchi, Y. Saeki, Y. Sato, and M. Furusawa.** 1985. Production of human α-interferon in silkworm using a baculovirus vector. Nature (London) **315**:592–594.
23. **Maeda, S., and K. Majima.** 1990. Molecular cloning and physical mapping of the genome of *Bombyx mori* nuclear polyhedrosis virus. J. Gen. Virol. **71**:1851–1855.
24. **Maeda, S., Y. Mukohara, and A. Kondo.** 1990. Characteristically distinct isolates of the nuclear polyhedrosis virus from *Spodoptera litura*. J. Gen. Virol. **71**:2631–2639.
25. **Maeda, S., S. L. Volrath, T. N. Hanzlik, S. A. Harper, K. Majima, D. W. Maddox, B. D. Hammock, and E. Fowler.** 1991.

Insecticidal effects of an insect-specific neurotoxin expressed by a recombinant baculovirus. Virology **184:**777–780.
26. **Maniatis, T., E. F. Fritsch, and J. Sambrook.** 1982. Molecular cloning: a laboratory manual. Cold Spring Harbor Laboratory, Cold Spring Harbor, N.Y.
27. **Miller, L. K.** 1988. Baculoviruses as gene expression vectors. Annu. Rev. Microbiol. **42:**177–199.
28. **Nagamine, T., H. Sugimori, K. Nakamura, S. Saga, and M. Kobayashi.** 1991. Nucleotide sequence of the gene coding for p40, an occluded virion-specific polypeptide of *Bombyx mori* nuclear polyhedrosis virus. J. Invertebr. Pathol. **58:**290–293.
29. **Nissen, M. S., and P. D. Friesen.** 1989. Molecular analysis of the transcriptional regulatory region of an early baculovirus gene. J. Virol. **63:**493–503.
30. **Oellig, C., B. Happ, T. Muller, and W. Doerfler.** 1987. Overlapping sets of viral RNAs reflect the array of polypeptides in the *Eco*RI J and N fragments (map positions 81.2 to 85.0) of the *Autographa californica* nuclear polyhedrosis virus genome. J. Virol. **61:**3048–3057.
31. **Ooi, B. G., C. Rankin, and L. K. Miller.** 1989. Downstream sequences augment transcription from the essential initiation site of a baculovirus polyhedrin gene. J. Mol. Biol. **210:**721–736.
32. **Possee, R. D., T. P. Sun, S. C. Howard, M. D. Ayres, M. Hill-Perkins, and K. L. Gearing.** 1991. Nucleotide sequence of the *Autographa californica* nuclear polyhedrosis virus 9.4 kbp EcoRI-I and -R (polyhedrin gene) region. Virology **185:**229–241.
33. **Rankin, C., B. G. Ooi, and L. K. Miller.** 1988. Eight base pairs encompassing the transcriptional start point are the major determinant for baculovirus polyhedrin gene expression. Gene **70:**39–49.
34. **Rohrmann, G. F.** 1986. Polyhedrin structure. J. Gen. Virol. **67:**1499–1513.
35. **Rohrmann, G. F.** 1992. Baculovirus structural proteins. J. Gen. Virol. **73:**749–761.
36. **Stewart, L. M. D., M. Hirst, M. L. Ferber, A. T. Merryweather, P. J. Cayley, and R. D. Possee.** 1991. Construction of an improved baculovirus insecticide containing an insect-specific toxin gene. Nature (London) **352:**85–88.
37. **Tomalski, M. D., and L. K. Miller.** 1991. Insect paralysis by baculovirus-mediated expression of a mite neurotoxin gene. Nature (London) **352:**82–85.
38. **Vlak, J. M., A. Schouten, M. Usmany, G. J. Belsham, E. C. Klinge-Roode, A. J. Maule, W. M. VanLent, and D. Zuidema.** 1990. Expression of cauliflower mosaic virus gene I using a baculovirus vector based upon the p10 gene and a novel selection method. Virology **179:**312–320.
39. **Whitford, M., and P. Faulkner.** 1992. Nucleotide sequence and transcriptional analysis of a gene encoding gp41, a structural glycoprotein of the baculovirus *Autographa californica* nuclear polyhedrosis virus. J. Virol. **66:**4763–4768.